Numerical simulation of asymmetric hurricanes on a β-plane with vertical shear[1]

By RANGARAO V. MADALA,[2] *Geophysical Fluid Dynamics Institute, Florida State University, Tallahassee, Florida 32306, USA* and
STEVE A. PIACSEK, *Naval Research Laboratory, Washington, D.C. 20375, USA*

(Manuscript received February 26; in final form December 12, 1974)

ABSTRACT

A three-layer, semi-implicit model was developed to simulate moving and asymmetric hurricanes on a β-plane, using Kuo's method of cumulus parametrization. Sensible and latent heat transfer from ocean to atmosphere was included implicitly in the model. In order to predict hurricane movement over a large area and yet resolve finer details near the eye, a multi-grid network was used with a movable finest grid of 20 km mesh size, surrounded by two coarse grid nets with mesh spacings of 60 km and 180 km, respectively. A comparison of the results with f-plane calculations shows that the vortex on the β-plane intensified at a slower rate before the storm stage, but at the same rate thereafter. The β-plane hurricane was asymmetric throughout its life cycle, and these asymmetrics looked similar to those observed in real hurricanes. The vortex moved on the β-plane with a phase velocity of 4.3 km hour^{-1} for the westerly and 3.3 km hour^{-1} for the northerly components. The model was also integrated for two cases where the initial vortex was superimposed on a vertically varying basic current. Results showed that the strength of the simulated hurricane depends very much upon the magnitude of the vertical shear of the basic current; for a large shear ($\geqslant 15$ m sec^{-1}/12 km) the vortex failed to intensify into a hurricane. Computations showed that the pressure weighted mean of the basic current between the surface and 12 km level agreed very well with the magnitude of the steering current. As a result of the interaction between the hurricane circulation and the basic current, the hurricane moved in an oscillatory path with an amplitude of 30 km and a period of about 20 hours.

I. Introduction

In the last decade or so, several workers have successfully simulated numerically the growth and development of hurricanes, using the crucial technique of cumulus parameterization developed by Kuo (1965), Ogura (1964) and Ooyama (1969). Axisymmetric models were developed by Yamasaki (1968*a* and *b*), Rosenthal (1969) and Sundquist (1970). Even though these models simulated some of the observed features of real hurricanes, they could not simulate asymmetries such as the confluence and diffluence lines in the streamline fields, the cloud bands and the motion of the hurricanes. Also, inhibiting mechanisms such as a vertical shear in the basic current could not be included in these models.

Anthes et al. (1971) simulated an asymmetric hurricane on an f-plane by integrating a three layer primitive equation numerical model over a grid system of uniform grid length (30 km) inside a circular region of radius 450 km. They used as initial conditions a balanced symmetric vortex of moderate strength (maximum wind speed of 18 m sec^{-1}), with a cumulus parameterization similar to that of Yamasaki (1968*b*, 1969) and Rosenthal (1969). The model successfully simulated some of the observed features of real hurricanes, such as cloud bands and the asymmetries in the outflow layer. Since the model was integrated on an f-plane, and

[1] Contribution No. 108 of the Geophysical Fluid Dynamics Institute, Florida State University.

[2] Now at Science Applications, Inc., McLean, Va. 22101.

the vortex was not allowed to interact with other systems in the atmosphere, it produced only those asymmetries that resulted from the dynamic instability. Due to the limited horizontal extent of the model, it could not simulate asymmetries generated by mechanisms other than the dynamic instability and interaction of the hurricane with the surroundings.

Madala (1973) and Kurihara & Tuleya (1974) have also performed simulations on an f-plane employing variable meshes. Madala used three nested meshes, each of uniform spacing, with the inner two following the eye of the hurricane; the set up will be detailed later in Section II. Kurihara & Tuleya used a stationary, cylindrical mesh centered on the (non-moving) eye and stretched in the radial direction. Both obtained improved results on energy transformations, due to better resolution, which agreed well with observational budget analyses. The resultant hurricane structure exhibited many of the observed features of hurricanes.

Mathur (1974) also simulated an asymmetric hurricane on a plane with variable Coriolis parameter using a four level primitive equation numerical model. The domain of integration (1 760 km $\times$ 1 760 km) was about four times larger than the domain of integration used by Anthes et al. (1971). The model was integrated over a multigrid network consisting of fine grid spacing of 37 km near the center, surrounded by a coarse grid network with a grid length of 74 km. The fine and coarse grid networks occupied square regions with sides of 880 km and 1 760 km, respectively, and the latent heat parameterization followed that of Kuo (1965). The initial conditions for the model were obtained from the real data for hurricane Isbel, 1964, when it was in a tropical depression stage. The model simulated the asymmetries in the wind, temperature and pressure fields, and also the movement of the hurricane. It also simulated the cloud bands and the eye of the hurricane. The maximum surface wind reached a value of about 80 m sec^{-1} at the time (96 hours) the integration was terminated.

With the insight gained from these models, we proceeded to build the current model to gain further insight into some additional features associated with moving hurricanes. By halving the radial mesh intervals at the center, we obtained a better resolution of the important processes surrounding the eye of the hurricane. By using a coarse mesh roughly four times the size of previous meshes, we allowed a much greater degree of freedom for the movement of hurricanes. By successively including the effects of an f-plane, β-plane and uniform zonal current with vertical shear, we obtained a better understanding of the contribution of each of these effects to the asymmetries and movements of three-dimensional, realistic hurricanes. Finally, the use of a semi-implicit method of time integration has reduced the overall computational time requirements by a factor of four, over previously used explicit methods, enabling one to study more cases for the same computational effort. The model was integrated on a multi-grid system. The grid system contained a finest grid network with a grid length of 20 km near the center of the simulated hurricane. The finest grid was surrounded by two coarse grid networks called fine and coarse with grid lengths of 60 km and 180 km. The finest and fine grid networks occupied a square region of side 520 km and 1 560 km, respectively; whereas the coarse grid network occupied a rectangular region of 9 350 km and 2 520 km. A semi-implicit time integration was used to save the computing time. The latent heat released in the cumulus clouds was parameterized in a manner similar to that described by Rosenthal (1969) and Yamasaki (1968*a*, 1969).

Gray (1967) hypothesized that a large vertical shear of the basic wind can inhibit the intensification of a tropical disturbance embedded in it. To test this hypothesis, the model was integrated in two cases from initial conditions that included a vertically varying basic current of differing magnitudes. The results are given in Section IV.

II. The basic equations and the numerical model

2.1. *Basic equations*

The basic equations (see Appendix A for list of symbols) governing the model in a Cartesian coordinate system are

$$\frac{\partial \varrho_0 u}{\partial t} + \frac{\partial \varrho_0 u^2}{\partial x} + \frac{\partial \varrho_0 uv}{\partial y} + \frac{\partial \varrho_0 uw}{\partial z} - f\varrho_0 v = -\varrho_0 \theta \frac{\partial \phi}{\partial x} + \frac{\partial \tau_{xx}}{\partial x} + \frac{\partial \tau_{yx}}{\partial y} + \frac{\partial \tau_{zx}}{\partial z} \quad (1)$$

$$\frac{\partial \varrho_0 v}{\partial t} + \frac{\partial \varrho_0 uv}{\partial x} + \frac{\partial \varrho_0 v^2}{\partial z} + \frac{\partial \varrho_0 vw}{\partial z} + f\varrho_0 u = -\varrho_0 \theta \frac{\partial \phi}{\partial y} + \frac{\partial \tau_{xy}}{\partial x} + \frac{\partial \tau_{yy}}{\partial y} + \frac{\partial \tau_{zy}}{\partial z} \quad (2)$$

$$\frac{\partial \phi}{\partial z} = \frac{g}{\theta} \quad (3)$$

$$\frac{\partial \varrho_0 u}{\partial x} + \frac{\partial \varrho_0 v}{\partial y} + \frac{\partial \varrho_0 w}{\partial z} = 0 \quad (4)$$

$$\frac{\partial \varrho_0 \theta}{\partial t} + \frac{\partial \varrho_0 u\theta}{\partial x} + \frac{\partial \varrho_0 v\theta}{\partial y} + \frac{\partial \varrho_0 \theta w}{\partial z} = \frac{\varrho_0 H}{\phi} + \frac{K_H \varrho_0 C_p \nabla_H^2 \theta}{\phi} \quad (5)$$

and

$$\theta\phi = C_p T \quad (6)$$

Eqs. (1) and (2) are the equations of motion in momentum form for the horizontal components of velocity. Since the horizontal dimension of a hurricane is at least two orders of magnitude larger than the vertical dimension, the equation of motion for the vertical component of momentum can be simplified into the hydrostatic equation given by (3). Eq. (4) is a simplified form of the continuity equation. Use of this form of the continuity equation to simulate the life cycle of a hurricane can be justified by a scale analysis. Eq. (5) is the thermodynamic equation.

The horizontal and vertical momentum flux terms in eqs. (1) and (2) are assumed to be of the following form:

$$\tau_{xx} = \varrho_0 K_H \frac{\partial u}{\partial x},\ \tau_{yx} = \varrho_0 K_Z \frac{\partial u}{\partial z},\ \tau_{zx} = \varrho_0 K_Z \frac{\partial u}{\partial z},$$

$$\tau_{xy} = \varrho_0 K_H \frac{\partial v}{\partial x},\ \tau_{yy} = \varrho_0 K_H \frac{\partial v}{\partial y},\ \tau_{zy} = \varrho_0 K_Z \frac{\partial v}{\partial z}$$

and at the surface

$$\tau_{zx} = \varrho_0(1)\, C_D u_1 (u_1^2 + v_1^2)^{1/2},$$

$$\tau_{zy} = \varrho_0(1)\, C_D v (u_1^2 + v_1^2)^{1/2}$$

where K_H, K_Z are, respectively, the horizontal and the vertical eddy coefficients of viscosity, C_D the drag coefficient, $\varrho_0(1)$ the density of air at the surface in the mean tropical atmosphere and u_1, v_1 are the horizontal components of the velocity at the 0.5 km level in the numerical model.

Table 1. *Values of the various parameters used in the model*

Parameter	Value
K_H	10^8 cm² sec⁻¹
C_D	3.0×10^{-3}
k_Z	10^5 cm² sec⁻¹ at level 3
	5.0×10^4 cm² sec⁻¹ at level 5

Hawkins & Rubsam (1968) estimated the values of the drag coefficient, C_D, from the data of the hurricane Hilda, 1964. The estimated values range from 1.2×10^{-3} to 3.6×10^{-3} with a curvilinear dependence on the wind speed. In the present model, the value of C_D was kept constant with a value of 3×10^{-3}, which is approximately the mean value of the drag coefficients obtained by Hawkins & Rubsam (1968) for the wind speeds between 30 m sec^{-1} and 60 m sec^{-1}. The horizontal eddy coefficient, K_H, was held constant for all time during the integration with a value of 10^8 cm sec^{-1} and was the same for momentum and heat. This is slightly higher than the estimates of Riehl & Malkus (1961) from the hurricane Daisy, 1958. The vertical eddy coefficient of viscosity, K_z, assumed to vary linearly with height with a value of 10^5 cm^2 sec^{-1} at the surface and zero at the top. Vertical diffusion of heat was not included in the model because of relatively insufficient knowledge about the behaviour of the vertical flux of heat in a hurricane.

The sensible heat transfer between the hurricane and the ocean surface was included implicitly in the model by assuming that the temperature at the levels 1 and 2 of the model (Fig. 1) were constant for all time. In other words, the in-spiralling air was assumed to undergo an isothermal expansion. Hawkins & Rubsam (1968) verified the isothermal expansion by estimating the surface temperatures of the hurricane Hilda, 1964.

Riehl & Malkus (1961) estimated from the data of hurricane Daisy, 1958 that the equivalent potential temperature of the in-spiralling air increased by about 10°C from 350°K to

		Z HEIGHT (KM)	LEVEL
	$\rho_o(7)$ $\rho_o(7)w_3=0$ $k_z\frac{\partial v}{\partial z}=k_z\frac{\partial U}{\partial z}=0$	17.0	7
LAYER 3	$\rho_o(6)$ $u_3, v_3, \phi_3, \theta_3, T_3$	12.0	6
	$\rho_o(5)$ w_2	7.0	5
LAYER 2	$\rho_o(4)$ $u_2, v_2, \phi_2, \theta_2, T_2$	4.0	4
	$\rho_o(3)$ w_1	1.0	3
LAYER 1 (SURFACE BOUNDARY LAYER)	$\rho_o(2)$ $u_1, v_1, \phi_1, \theta_1, T_1 = 296.6°K$	0.5	2
	$\rho_o(1)$ $\phi_o, \theta_o, T_o = 299.9°K$; $\rho_o(1)w_o = 0$	0	1

Fig. 1. The three layer numerical model.

360°K when the minimum surface pressure reached a value of 950 mb. The present model includes the latent heat transfer by assuming that a parcel rises dry-adiabatically from the surface till it reached a temperature of 23.6°C and saturated adiabatically thereafter. Since the temperatures at the levels 1 and 2 of the model (Fig. 1) were held constant during the integration, the above assumption gives a constant value of about 400 meters for the height of the lifting condensation level (or the cloud base). Therefore, the equivalent potential temperature of the air rising in the cumulus clouds depends only upon the pressure at the cloud base. It increases from the initial value of 349°K to about 359°K when the minimum surface pressure reaches 953 mb. These values compare favorably with the observations of Riehl & Malkus (1961). This assumption eliminated the need of having a water transport equation.

The first term on the right side of the thermodynamic equation represents diabatic heating. In the present model, this term included only the latent heat released due to condensation of water vapor in "tall" cumulus clouds.

2.2. *The three layer model and the grid system*

As shown in Fig. 1, the numerical model contained three layers in the vertical. The lowest layer is the surface boundary layer and the top layer contained most of the upper troposphere. Since a major part of the inflow in a hurricane occurs in the lower boundary layer and the outflow in the upper troposphere, these two layers of the model can be called the inflow

Table 2. *Approximate values of pressure, density, and potential temperature in the mean tropical atmosphere (Jordan, 1959) at various levels of the model*

Level	Height (km)	Pressure (mb)	Potential temperature (θ_0) (°K)	Density (ϱ_0) (10^{-3} g cm^{-3})
1	0.0	1 015	298.3	1.167
2	0.5	959	300.3	1.116
3	1.0	906	302.3	1.068
4	4.0	634	316.3	0.795
5	7.0	433	329.3	0.581
6	12.0	214	344.3	0.337
7	17.0	93	397.3	0.161

and the outflow layers. The middle layer is characterized by strong tangential velocities with no pronounced radial mass flux. The variables were staggered both in the horizontal and the vertical directions. The horizontal velocity components u and v were specified at levels 2, 4, and 6 (Fig. 1). The thermodynamic variables θ and ϕ were specified at levels 1, 2, 4, and 6, the vertical velocity, w, was specified at levels 1, 3, 5, and 7. Corresponding values of pressure, density and potential temperature in the mean tropical atmosphere (Jordan, 1958) are given in Table 2.

The horizontal and vertical grid arrangement for the dependent variables are given in Figs. 2 and 1, respectively; the grid system is similar to the one used by Williams (1969). The rapid variation of the dependent variables near the center of a hurricane necessitated the use of a grid telescoping technique, with a fine mesh of 20 km near the center, surrounded by two coarse grid networks with mesh sizes of 60 km and 180 km, respectively (see Fig. 3). Hereafter we will refer to these three as the finest, fine, and coarse grid networks, respectively.

2.3. *The semi-implicit time integration method*

In explicit time integration of the primitive equations the fast moving internal gravity waves allow only a very small time step in the CFL (Courant-Friedrichs-Lewy) condition so that a resource to implicit (Kurihara, 1965) or semi-implicit (Kwizak & Robert, 1971) schemes must be taken. The semi-implicit method developed by Kwizak & Robert (1971) treats implic-

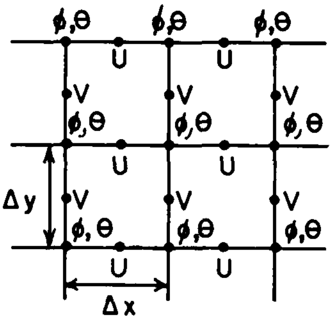

Fig. 2. Grid network in $x-y$ plane.

itly only the terms in the equations of motion which govern the gravity waves and calculates all other terms explicitly, thereby shifting the dependence of the time step from the speed of the gravity waves to the speed of the meteorological waves. The increase in the time step through the use of the semi-implicit method will not affect the accuracy of the results since the time truncation errors will be still smaller than the space truncation errors. This method was successfully used by Kwizak & Robert (1971) and McPherson (1971) for barotropic models and Robert et al. (1972) for a baroclinic model. The semi-implicit method used in the present model (which is described in Appendix B) was similar to the one described by Robert et al. (1972).

In the present model, an initial step of 900 seconds was used (about 20 times the step allowed for an explicit scheme). The time step was gradually reduced to 60 seconds as the hurricane intensified and reached a mature stage.

2.4. *Diabatic heating*

The quantity H in the thermodynamic eq. (5) represents diabatic heating per unit mass. In

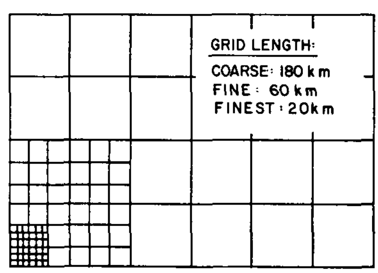

Fig. 3. The multi-grid network in $x-y$ plane.

the present model, this term only includes the latent heat released due to condensation of water vapor in "tall" cumulus clouds. Whenever there was a convergence of mass in the boundary layer and the air was conditionally unstable in the lower troposphere, we assumed that the water vapor converging in the boundary layer rose in tall cumulus clouds, condensed, and fell as precipitation. We also assumed that all the latent heat released in the cumulus clouds was available for increasing the temperature of the hurricane scale circulation.

The temperature distribution in the cumulus clouds (cloud temperature) was assumed to be equal to the temperature of a parcel of air rising from the surface along a dry adiabat till the temperature reached a value of 23.6°C, and along a saturated adiabat thereafter. From these three assumptions we obtained the following expression for the total amount of latent heat, H, released due to condensation of water vapor in cumulus clouds:

$$H = \varrho_0(3) w_1 L q_s(T = 23.6°\text{C}, \phi_l) \quad \text{If } w_1 > 0 \text{ and } T_c > T$$
$$= 0 \quad \text{otherwise}$$

where $q_s(T = 23.6°\text{C}, \phi_l)$ is the saturation mixing ratio of a parcel of air at the lifting condensation level, L is the latent of condensation and T_c is the cloud temperature. Since the model predicted the temperature only in layers 2 and 3, we assumed that the total latent heat, H, released in the cumulus clouds was distributed between these two layers in such a way that the amount of heat available to each layer is proportional to the difference of cloud temperature and the temperature of the hurricane scale circulation. Hereafter, we refer to the difference between the cloud temperature and the temperature of the hurricane scale circulation as the temperature anomaly. The amount of latent heat released per unit mass in layer 2 is

$$H_1 = \frac{H(T_c(4) - T_2)}{\Delta} \quad \text{If } T_c(4) > T_2$$
$$= 0 \quad \text{otherwise,}$$

and the amount of latent heat released per unit mass in layer 3 is

$$H_2 = \frac{H(T_c(6) - T_3)}{\Delta} \quad \text{If } T_c(6) > T_3$$
$$= 0 \quad \text{otherwise,}$$

where $T_c(4)$ and $T_c(6)$ were the cloud temperatures at levels 4 and 6, respectively, and $\Delta = \varrho_0(4)\,\Delta z_2(T_c(4) - T_2) + \varrho_0(6)\,\Delta z_3(T_c(6) - T_3)$. This formulation is similar to the one used by Rosenthal (1969) and Yamasaki (1968*a*, 1968*b*, 1969).

III. Initial conditions

Time integration of the numerical model described in the last section was carried out on a β-plane centered at 20° N with a weak, axisymmetric and barotropic vortex in a gradient wind balance as the initial conditions. The tangential velocity of this vortex was taken to be a function of radius only, and was given by

$$v = v_{\max}\left(\frac{r}{r_0}\right) e^{1/2}\left(1 - \left(\frac{r}{r_0}\right)^2\right) \tag{7}$$

where v was the tangential velocity, $v_{\max}$ and r_0 were the magnitude and the radius of the maximum tangential velocity respectively. In the present model, the values of $v_{\max}$ and r_0 were taken to be 4 m sec^{-1} and 360 km, respectively. The functional form of the initial conditions is the same as the one taken by Sundqvist (1970) for his ten level symmetric model.

The pressure distribution that balances the wind distribution given by the eq. (7) was obtained by solving the gradient wind equation, given by

$$\frac{v^2}{r} + fv = \theta\frac{\partial\phi}{\partial r} \tag{8}$$

with the help of the equation of state $\theta\phi = C_p T$, eq. (8) was written in the following form,

$$\frac{v^2}{r} + fv = C_p T\frac{\partial \ln \phi}{\partial r} \tag{9}$$

This equation was solved for the distribution of ϕ by assuming that the temperature was constant on any horizontal level and equal to the temperature of the mean tropical atmosphere at that level.

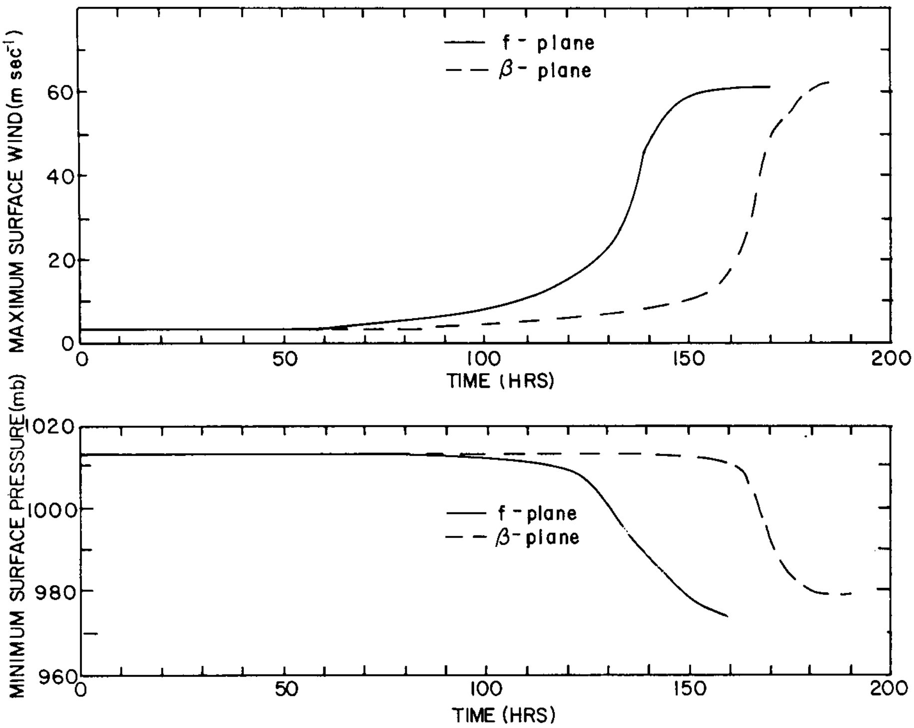

Fig. 4. Time variation of minimum surface pressure (bottom) and maximum surface wind (top) on f- and β-planes.

To test the effect of a vertically sheared mean current, we included a basic E-W current in geostrophic balance upon which the vortex was superimposed.

IV. Results of the numerical integration

The model described in Section II has been used in a study by Madala (1973) to obtain results with an f-plane integration. The relevant results from this study, i.e., results which will be needed to exhibit the effects of the β-plane and the presence of a uniform, vertically sheared current, will be included for comparison in the respective figures and tables displaying results from the current β-plane and shear calculations. Time variation of the minimum surface pressure obtained from both the f- and β-plane integrations is given in Fig. 4. The figure clearly shows that the vortex intensified at a slower rate on the β-plane than on the f-plane before it reached a storm stage, and at the same rate thereafter. A plausible explanation for this phenomenon is given below.

During the first 170 hours, the vortex moved a total distance of 1 016 km (Curve II of Fig. 5) giving an average phase speed of 6.0 km hour^{-1}. This long movement due to the β-effect resulted in the advection of part of the released latent heat out of the region of low level convergence, and hence in the generation of weaker temperature gradients in the middle and upper tropospheres than its f-plane counterpart. Since the vortex is in hydrostatic balance, these gradients produced smaller surface pressure gradients on the β-plane, thereby intensifying the vortex at a slower rate. After the vortex reached the storm stage, its phase speed was reduced to less than 3 km hour^{-1}, and the storm intensified at the same rate on both planes.

The β-plane hurricane was asymmetric throughout its life cycle. These asymmetries resemble closely those observed in real hurricanes, and are stronger than those formed by the release of the hydrodynamic instability

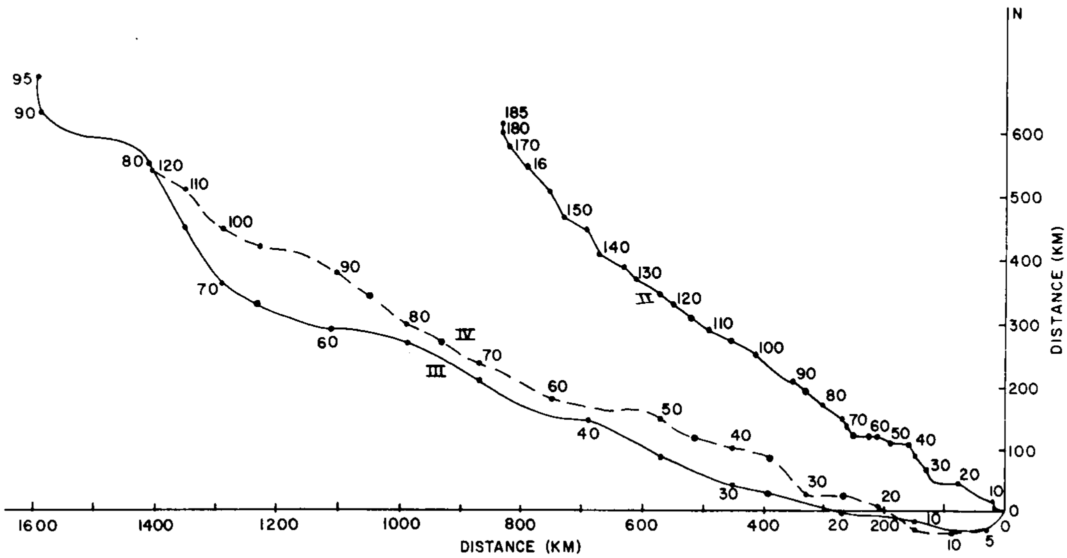

Fig. 5. Path of the simulated hurricane in cases II, III, and IV. The simulated hurricane was nearly stationary in case I. The numbers along the curve are the time of integration (in hours).

during the mature stage of the f-plane hurricane. In order to understand their three dimensional structure, the results at 175 hour (mature stage) were analyzed and are given below.

The streamline and isotach analysis of the flow at 175 hour for the 0.5 km and 12.0 km levels are given in Figs. 6 to 9. The confluence lines at the 0.5 km level and the diffluence lines at the 12.0 km level in the streamline fields can be clearly seen in these figures. The wind speeds were higher in the NE sector and lower in the SW sector. The maximum wind speed at the 0.5 km level was about 58 km sec^{-1} and at the 12 km level was about 30 m sec^{-1}. The vertical

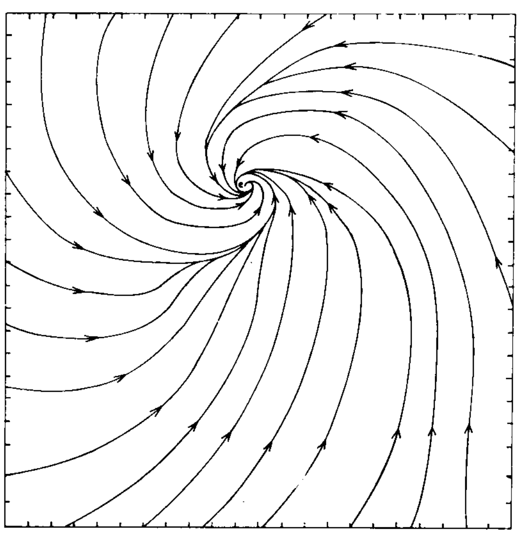

Fig. 6. Streamline analysis of 0.5 km level at 175 hour (β-plane model).

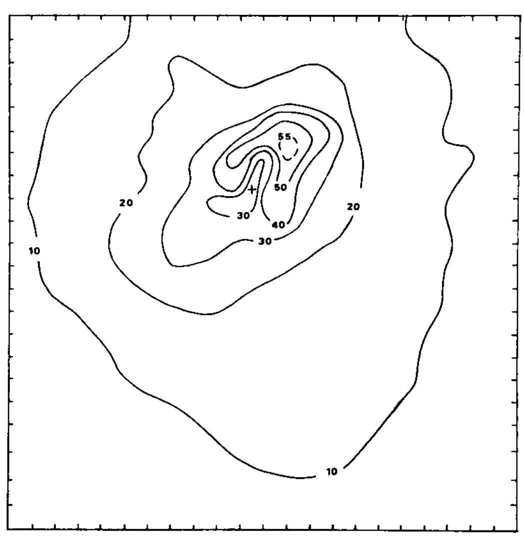

Fig. 7. Isotach analysis of 0.5 km level at 175 hour (β-plane model). Units: m sec^{-1}.

velocities (not shown here) were higher in the NE sector. The sinking motion at the center penetrated the upper and (most of) the lower troposphere. The upward motion was concentrated in two major and two minor (spiral) bands separated by areas of descending motion.

The path of the hurricane is given in Curve II of Fig. 5 with the time of integration (in hours) given to the right of the path. Both the E–W and N–S components of the phase velocity increased with time before the storm stage, and decreased thereafter. The vortex changed its direction from the initial WNW to NW during the first 120 hours and NNW after 160 hours. As expected from the Bjerknes–Holmboe theory, the hurricane moved from East to West due to the β-effect. Rossby (1948) gives the northward force, F, acting on a symmetric isolated vortex as:

$$F = M\beta\bar{\omega}\,\frac{R^2}{4} \tag{1}$$

where R is the radius of the outer boundary, M is the total mass and $\bar{\omega}$ is the relative angular velocity averaged over the vortex. This force results from a lack of local balance between the pressure gradient, Coriolis and centrifugal forces. Since the vortex is assumed to be isolated, there are no outside pressure forces in the environment to enter into this balance, and the vortex would experience a northward acceleration when its overall circulation was cyclonic ($\bar{\omega} > 0$, and southward if it was anti-cyclonic ($\bar{\omega} < 0$). However, real hurricanes are asymmetric and interact with the environment so that they adjust their shapes to achieve a near local gradient wind balance. Thus, eq. (1) overestimates the force F and resulting speed for a hurricane. However, this equation can be used to explain qualitatively the northward movement of the hurricane on the β-plane.

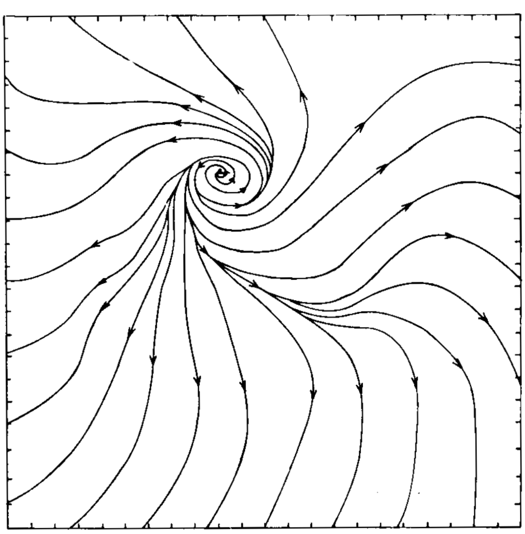

Fig. 8. Streamline analysis of 12.0 km level at 175 hour (β-plane model).

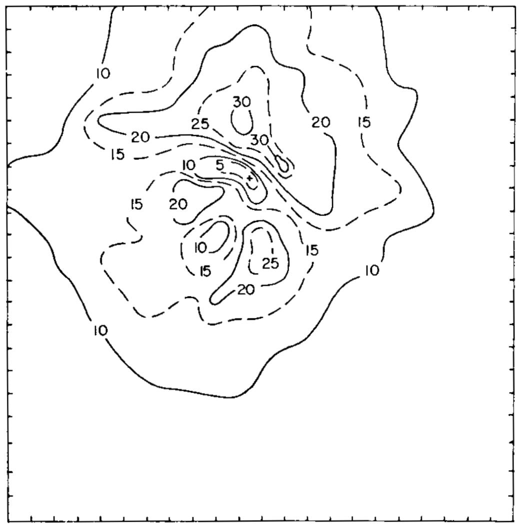

Fig. 9. Isotach analysis of 12.0 km level at 175 hour (β-plane model). Unit: m sec^{-1}.

In a hurricane, the magnitude of $\bar{\omega}$ depends upon the relative strengths of the low level cyclonic circulation and the upper level anti-cyclonic circulation. Since the anti-cyclonic circulation was either weak or absent during the first 170 hours, is positive and the vortex experienced a northward acceleration. This can be seen in curve II of Fig. 5 as an increase in the northward component of the phase velocity with time. After 170 hours, due to the increased strength of the upper tropospheric anti-cyclonic circulation, the vortex experienced a northward deceleration. During the first 190 hours of integration, the vortex moved a distance of 825 km towards West and 625 km towards North, giving an average speed of 4.3 km $hour^{-1}$ for the westerly components and 3.3 km $hour^{-1}$ for the northerly components, respectively.

The model was also integrated for two cases

Table 3. *Magnitude of the basic current at the three levels of the model and the maximum mean tangential wind speed obtained from the integration of the model in all the four cases*

Case	Basic current cm sec^{-1} Level (km) 0.5	4.0	12.0	Maximum mean tangential velocity obtained from the integration (m sec^{-1})
I (f-plane)	0	0	0	53
II (β-plane)	0	0	0	46
III (β-plane)	0	−500	−1 500	20
IV (β-plane)	0	−330	−1 000	33

where the initial vortex was superimposed on a vertically varying basic current. The magnitude of the basic current at the three levels of the model, and the maximum azimuthally averaged tangential wind speed v_θ obtained from the integration, are given in Table 3. The time variation of v_θ is given in Fig. 10.

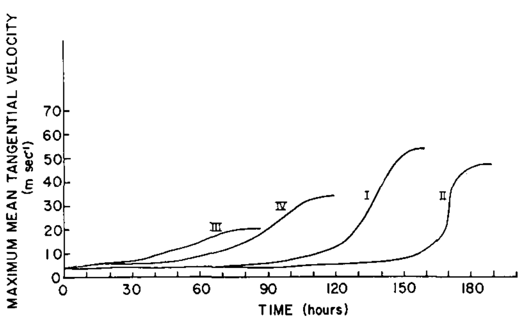

Fig. 10. Time variation of the maximum mean tangential velocity in all four cases.

It can be seen from the table that the strength of the simulated hurricane depends very much upon the magnitude of the initial vertical wind shear of the basic current. For large wind shear (≥ 15 m sec^{-1}) the vortex failed to intensify into a hurricane.

The mean potential temperature ($\bar{\theta}$) anomalies at the 12 km level are given in Fig. 11 as a function of radius. The figure shows that $\bar{\theta}$ varied very rapidly between the 30 km and

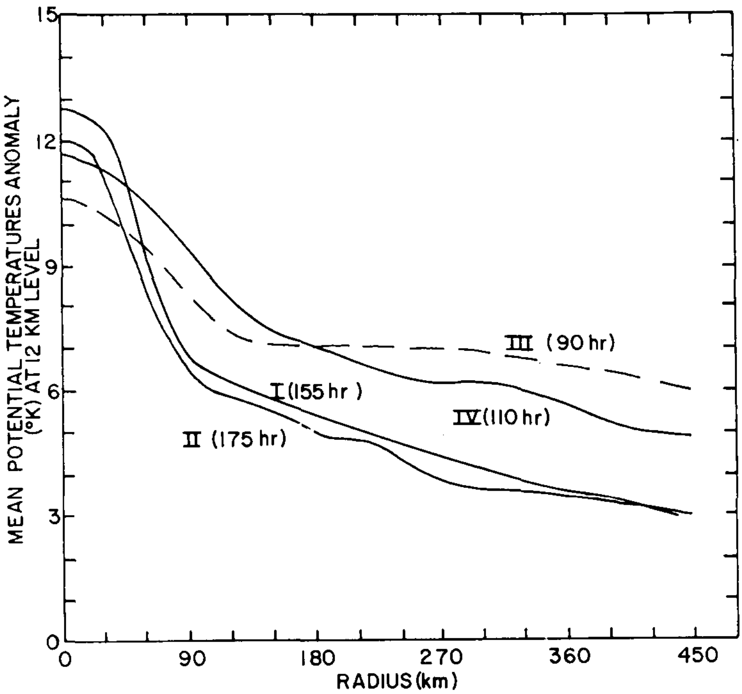

Fig. 11. Mean potential temperature anomaly (°C) in all four cases. Level: 12 km.

Table 4. *Easterly component of the phase speeds and the deviation of the phase speeds from the basic current (units: km hour^{-1})*

Case	Basic current (U) at 12.0 km level	Easterly component of the phase speed (C)	$\|U-c\|$
I	0	0	0
II	0	−4	4
III	−54	−18	36
IV	−36	−12	24

90 km radii in the cases in which the vortex intensified into a hurricane, and less rapidly in the other case. It must also be noted that the potential temperature averaged over a circular area of radius 450 km was nearly the same in all cases. The weak temperature gradients obtained in the cases of large vertical shears resulted from a strong advection of the released latent heat from the area of low level convergence to the surroundings. The case in which the shear was 15 m sec^{-1}, the surface pressure gradients were weaker than those necessary to balance hurricane force winds, and thereafter the vortex failed to intensify into a hurricane.

Paths of the vortex in cases II, III, and IV are given in Fig. 5. The vortex was nearly stationary in case I, and moved in case II mainly under the influence of the β-effect. On the other hand, the vortex moved in cases III and IV under both the influence of the β-effect and the basic current. If we assume that the phase velocity of the vortex due to the β-effect is the same in all cases, then we can obtain the phase velocity of the vortex due to the basic current (also called the steering velocity) by subtracting the velocity of the vortex on the β-plane from the velocity of the vortex in cases III and IV. Observations (Jordan, 1952) showed that the magnitude of the steering current can be approximated by the pressure weighted mean of the basic current. To test this, the phase velocity, the magnitude of the steering current and the pressure weighted mean of the basic current between the surface and the 12 km level were computed for the cases III and IV, and are given in Tables 4 and 5. These tables show that the pressure weighted mean of the basic current agrees very well with the magnitude of the steering current.

We have seen so far the influence of the β-effect (an internal force) and the basic current (an external force) in determining the path of a hurricane. Yeh (1950) describes another internal force that can influence the path of a hurricane by producing oscillations of amplitude 30 km to 60 km and periods of 12 hours to 3 days. This force arises from the non-linear interaction of a vortex with the basic current. He obtained an analytical expression for the path of a Rankin vortex superimposed on a basic current, and showed that it follows an oscillatory (a trochoid) path. Due to the small amplitudes of these oscillations, it is difficult to observe them (if they occur) in real hurricanes. Yeh (1950) gives two examples of the oscillatory path of hurricanes (these are given in Fig. 12). Also, Cressman (1951) observed that the hurricane Doris (1950) followed an oscillatory path similar to the trochoid described by Yeh (1950). Oscillations of amplitude about 30 km and period of about 20 hours in the path of the vortex in cases III and IV can be clearly seen in Fig. 5.

Table 5. *Magnitude of the steering current and the pressure weighted mean of the basic current in the vertical*

Case	Easterly component of the phase speed C (km hour^{-1})	Deviation of C from the easterly component of the phase velocity of the vortex on the β-plane[a] (km hr^{-1})	Basic current U (km hour^{-1}) 0.5	4.0	12.0	$\frac{1}{P_B-P_T}\int_{P_B}^{P_T} U dP$ (km hour^{-1})
III	−18	−14	0	−18	−54	−13
IV	−12	−8	0	−12	−36	−9

[a] The easterly component of the phase velocity of the vortex on the β-plane is about −4 km hour^{-1}.

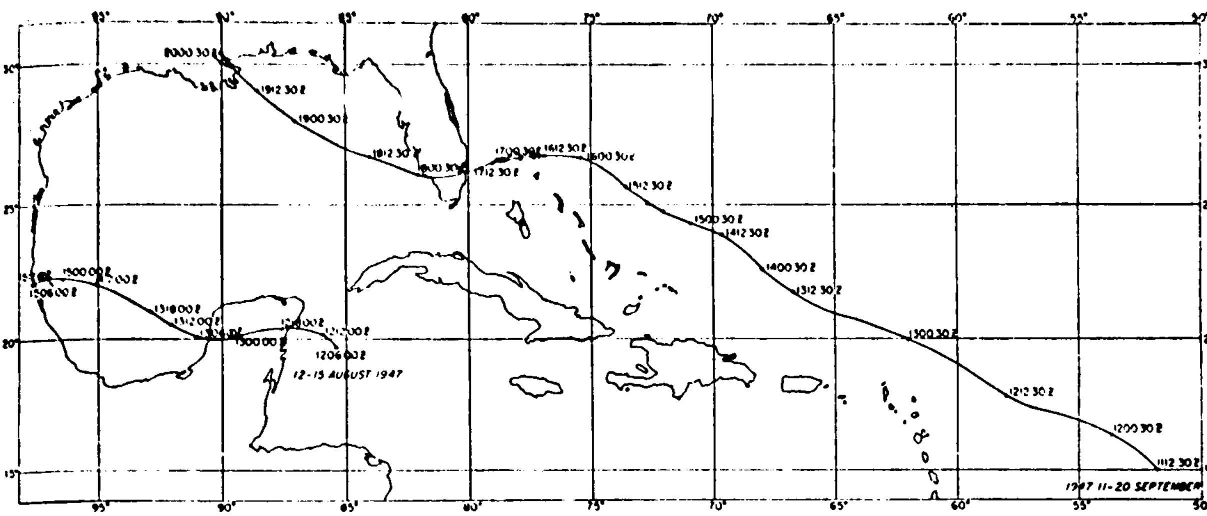

Fig. 12. Two examples of the oscillatory path of tropical storms (Yeh, 1950).

V. Conclusions

A three dimensional numerical model of the hurricane was integrated on a β-plane with a balanced weak vortex as the initial conditions. It was also integrated in two more cases with a vertically varying basic current superimposed on the vortex as the initial conditions. The important results obtained from these integrations are given below:

1. Asymmetries generated by the β-effect look similar to those observed in real hurricanes;
2. The β-effect moved the hurricane northward at an average speed of 3 km hour^{-1}. This speed was higher during the storm stage than during the mature stage;
3. CISK process alone can intensify a vortex into a hurricane only if the vertical shear of the basic current is less than 15 m sec^{-1};
4. The pressure weighted mean of the basic current between the surface and 12 km level can be used to estimate the magnitude of the basic current; and
5. The hurricane superimposed onto a basic current moves in an oscillatory path with deviatory amplitudes of 30 km and a period of about 20 hours.

Acknowledgements

This work is a part of the doctoral dissertation of the first author. He wishes to express his gratitude to Dr R. L. Pfeffer for his guidance and encouragement throughout this study. He was also benefited by the useful suggestions given by Dr J. J. O'Brien and Dr N. W. LaSeur. The authors wish to express their appreciation to Ms M. G. Schmidt for typing. Acknowledgement is made to the National Center for Atmospheric Research, which is sponsored by the National Science Foundation, for use of its computers (CDC 7600 and 6600) and the Florida State University computing center for use of its CDC 6500 computer. This work was supported by the Office of the Naval Research under grant N00014-68-A-0159.

Appendix A. List of symbols used in the model

C_D	Drag coefficient (assumed constant)
C_p	Specific heat capacity at constant pressure for dry air (= 1 004.64 × 10^4 erg g^{-1} deg^{-1})
f	Coriolis parameter
H	Heat added or removed per unit mass of air per unit time (diabatic heating)
K_H	Kinematic coefficient of eddy viscosity for horizontal mixing
K_Z	Kinematic coefficient of eddy viscosity for vertical mixing
P	Pressure
P_0	1 000 mb

q	Specific humidity
R	Specific gas constant for air (2.8704×10^6 erg g^{-1} deg^{-1})
T	Temperature
t	Time
u	Component of velocity in x direction (zonal velocity)
v	Component of velocity in y direction (meridional velocity)
w	Vertical velocity
x, y, z	Coordinate distances in the East–West, North–South, and in the vertical directions respectively
θ	Potential temperature $[= T(P_0/p)^{R/C_p}]$
ϕ	$= C_p(P/p_0)^{R/C_p}$
θ_e	Equivalent potential temperature
ϱ	Density
$\varrho_0 = \varrho_0(z)$	Density of the mean tropical atmosphere

Appendix B. The semi-implicit time integration method used in the model

For convenience we define the following finite difference operators:

$$\bar{F}^l = \frac{F(l-(\Delta l/2))+F(l+(\Delta l/2))}{2}$$

$$\delta_l F = \frac{F(l+(\Delta l/2))-F(l-(\Delta l/2))}{}$$

$$\bar{F}^{2l} = \frac{F(l-\Delta l)+F(l+\Delta l)}{2}$$

and

$$\delta_l^2 F = \delta_l(\delta_l F)$$

where F represents one of the dependent variables u, v, w, θ, or ϕ and $l(=x, y, z,$ or $t)$ represents one of the independent variables and Δl the grid interval in l.

In terms of a new thermodynamic variable $\alpha(\equiv 1/\theta)$, eqs. (1) to (6) take the following form

$$\frac{\partial \varrho_0 u}{\partial t} + \frac{\varrho_0}{\alpha}\frac{\partial \phi}{\partial x} = -A + \varrho_0 fv + \frac{\partial \tau_{xx}}{\partial x} + \frac{\partial \tau_{yx}}{\partial y} + \frac{\partial \tau_{zx}}{\partial z} \tag{B-1}$$

$$\frac{\partial \varrho_0 v}{\partial t} + \frac{\varrho_0}{\alpha}\frac{\partial \phi}{\partial y} = -B - f\varrho_0 u + \frac{\partial \tau_{xy}}{\partial x} + \frac{\partial \tau_{yy}}{\partial y} + \frac{\partial \tau_{zy}}{\partial z} \tag{B-2}$$

$$\frac{\partial \phi}{\partial z} = -g\alpha \tag{B-3}$$

$$\frac{\partial \varrho_0 u}{\partial x} + \frac{\partial \varrho_0 v}{\partial y} + \frac{\partial \varrho_0 w}{\partial z} = 0 \tag{B-4}$$

$$\frac{\partial \varrho_0 \alpha}{\partial t} - \frac{\partial \varrho_0 w\alpha}{\partial z} = \varrho_0 \frac{\alpha^2 H}{\phi} + C + \frac{\alpha^2 K_H \varrho_0 C_p}{\phi}\nabla_H^2 \theta \tag{B-5}$$

and

$$\phi = \alpha C_p T \tag{B-6}$$

where

$$A = \frac{\partial \varrho_0 u^2}{\partial x} + \frac{\partial \varrho_0 uv}{\partial y} + \frac{\partial \varrho_0 uw}{\partial z},$$

$$B = \frac{\partial \varrho_0 uv}{\partial x} + \frac{\partial \varrho_0 v^2}{\partial y} + \frac{\partial \varrho_0 uw}{\partial z}$$

and

$$C = \frac{\partial \varrho_0 u}{\partial x} + \frac{\partial \varrho_0 v}{\partial y}$$

The variable α can be separated into a basic part α_0 ($\equiv 1/\theta_0$) which is a function of only the vertical coordinate and a perturbation part $(\alpha - \alpha_0)$. The values of θ_0 at various levels of the model are given in Table 2. In terms of the basic part α_0 and the perturbation part $(\alpha - \alpha_0)$. Eqs. (B-1), (B-2), and (B-5) take the following form

$$\frac{\partial \varrho_0 u}{\partial t} + \frac{\varrho_0}{\alpha_0}\frac{\partial \phi}{\partial x} = -\varrho_0\left(\frac{1}{\alpha} - \frac{1}{\alpha}\right)\frac{\partial \phi}{\partial x} + A_1 + \varrho_0 fv \tag{B-7}$$

$$\frac{\partial \varrho_0 v}{\partial t} + \frac{\varrho_0}{\alpha_0}\frac{\partial \phi}{\partial y} = -\varrho_0\left(\frac{1}{\alpha} - \frac{1}{\alpha_0}\right)\frac{\partial \phi}{\partial y} + B_1 + \varrho_0 fu \tag{B-8}$$

and

$$-\frac{\partial \varrho_0 \alpha}{\partial t} - \frac{\partial \varrho_0 w\alpha_0}{\partial z} = \frac{\partial \varrho_0 w(\alpha - \alpha_0)}{\partial z} + \frac{\varrho_0 \alpha^2 H}{\phi} + C_1 \tag{B-9}$$

where

$$A_1 = -A + \frac{\partial\tau_{xx}}{\partial x} + \frac{\partial\tau_{yz}}{\partial y} + \frac{\partial\tau_{zx}}{\partial z}$$

$$B_1 = -B + \frac{\partial\tau_{xy}}{\partial x} + \frac{\partial\tau_{yy}}{\partial y} + \frac{\partial\tau_{zy}}{\partial z}$$

and

$$C_1 = C + \frac{\alpha^2 K_H C_p \varrho_0}{\phi} \nabla_H^2 \theta$$

Since weak gravity waves are governed by the pressure gradient force, vertical advection of potential temperature and divergence, the basic part of these terms are treated implicitly by applying central average in time and calculating all other terms in terms of the variables at time t. The finite-difference form of the Eqs. (B-7), (B-8), (B-9), (B-3), and (B-4) can be written in the following form.

$$\delta_t \overline{\varrho_0 u}^t + \frac{\varrho_0}{\alpha_0} \delta_x \overline{\phi}^{2t} = A_2 \tag{B-10}$$

$$\delta_t \overline{\varrho_0 v}^t + \frac{\varrho_0}{\alpha_0} \delta_y \overline{\phi}^{2t} = B_2 \tag{B-11}$$

$$\delta_t \overline{\varrho_0 \alpha}^t - \delta_z(\varrho_0 \overline{w}^{2t} \alpha_0) = C_2 \tag{B-12}$$

$$\delta_z \overline{\phi}^{2t} = -\overline{\overline{g\alpha}^{2t}}^{z} \tag{B-13}$$

and

$$\delta_x \overline{\varrho_0 u}^{2t} + \delta_y \overline{\varrho_0 v}^{2t} + \delta_z \overline{\varrho_0 w}^{2t} = 0 \tag{B-14}$$

where

$$A_2 = -\varrho_0 \overline{\left(\frac{1}{\alpha} - \frac{1}{\alpha_0}\right)}^{x} \delta_x \phi + A_1 + \varrho_0 f \overline{\overline{v}^{x}}^{y}$$

$$B_2 = -\varrho_0 \overline{\left(\frac{1}{\alpha} - \frac{1}{\alpha_0}\right)}^{y} \delta_y \phi + B_1 + \varrho_0 \overline{\overline{fu}^{x}}^{y}$$

and

$$C_2 = \delta_z(\overline{w\alpha - \alpha_0}^{z}) + \frac{\varrho_0 \alpha^2 H}{\phi} + C_2$$

The finite-difference form of the non-linear terms A, B, and C in eqs. (B-1), (B-2), and (B-5) will be discussed in the next section. Eqs. (B-10), (B-11), and (B-12) can also be written in the following form.

$$\overline{\varrho_0 u}^{2t} + \frac{\varrho_0}{\alpha_0} \Delta t \delta_x \overline{\phi}^{2t} = A_3 \tag{B-15}$$

$$\overline{\varrho_0 v}^{2t} + \frac{\varrho_0}{\alpha_0} \Delta t \delta_y \overline{\phi}^{2t} = B_3 \tag{B-16}$$

and

$$-\overline{\varrho_0 \alpha}^{2t} - \Delta t \delta_z(\varrho_0 \overline{w}^{2t} \alpha_0) = C_3 \tag{B-17}$$

where

$$A_3 = \Delta t A_2 + \varrho_0 u(t - \Delta t)$$

$$B_3 = \Delta t B_2 + \varrho_0 v(t - \Delta t)$$

and

$$C_3 = \Delta t C_2 - \varrho_0 \alpha(t - \Delta t)$$

From eqs. (B-14), (B-15), and (B-16) we can easily derive the following equation

$$\frac{\varrho_0}{\alpha_0} \Delta t(\delta_x^2 + \delta_y^2) \overline{\phi}^{2t} - \delta_z \overline{\varrho_0 w}^{2t} = \delta_x A_3 + \delta_y B_3 \tag{B-18}$$

With the help of eqs. (B-12) and (B-13), the term $\delta_z \overline{\varrho_0 w}^{2t}$ in eq. (B-18) can be written in terms of the dependent variables at time t and $\overline{\phi}^{2t}$ (see Madala, 1973 for details). The resulting equation will be an elliptic equation for $\overline{\phi}^{2t}$ and therefore can be solved by using a successive over relaxation technique. After solving eq. (B-18) for $\overline{\phi}^{2t}$, eqs. (B-10), (B-11), (B-12), and (B-14) can be solved, respectively, for $\bar{u}^{2t}$, $\bar{v}^{2t}$, $\bar{\alpha}^{2t}$, and $\overline{w}^{2t}$ and therefore for the values of the dependent variables at time $(t + \Delta t)$.

The same time step was used for integration on all three grid networks. The prognostic eqs. (B-15) to (B-17) were solved for each time step successively on the coarse, fine, and finest grid systems. The diagnostic eq. (B-18) for $\overline{\phi}^{2t}$ were solved by using the successive over relaxation technique. Each iteration during the relaxation process of eq. (B-18) consisted of sweeping successively the coarse, fine, and finest grid systems. Boundary conditions for the fine and the finest grid networks, for u, v, and θ at each time step and for $\overline{\phi}^{2t}$ for each iteration during the relaxation of eq. (B-18) were obtained by using Lagrangian interpolation from the forecasted values on the coarse and fine grid networks respectively. Boundary conditions for the coarse grid network were obtained by using upstream differencing.

Appendix C. Finite-difference form of the non-linear terms in the governing equations

The linear computational instability discussed in Section 2.3 and governed by the CFL condition results from the time truncation errors. The non-linear terms in the equations of motion can give rise to another kind of instability called non-linear instability. As shown by Lilly (1965) and Phillips (1959), this instability results from the misrepresentation of the short waves that are generated by the non-linear interactions and are small to be resolved by the grid system. Since this instability results from the space truncation errors, it can not be eliminated either by reducing the time step or by using the implicit or the semi-implicit methods described in Section 2.3. Arakawa (1966) and Lilly (1965) showed that this non-linear instability can be controlled by devising a finite-difference scheme which satisfies certain linear and quadratic integral constraints. The scheme used in this model has been described by Harlow & Welch (1965) and is equivalent to the J_2 scheme of Arakawa (1966).

The finite-difference form of A in Appendix B is

$$\varrho_0 \delta_x(\bar{u}^x \bar{u}^x) + \varrho_0 \delta_y(\bar{u}^y \bar{v}^x + \delta_z(\varrho_0 \bar{u}^z \overline{w}^x),$$

the finite-difference form of B in Appendix B is

$$\varrho_0 \delta_x(\bar{u}^y \bar{v}^x) + \varrho_0 \delta_y(\bar{v}^y \bar{v}^y) + \delta_2(\varrho_0 \bar{v}^z \overline{w}^y),$$

and the finite-difference form of C in Appendix B is

$$\varrho_0 \delta_x(\bar{\alpha}^x \bar{u}^x) + \varrho_0 \delta_y(\bar{\alpha}^y \bar{v}^y).$$

REFERENCES

Alaka, M. A. 1962. On the occurrence of dynamic instability in incipient and developing hurricanes. *Monthly Weather Rev. 90*, 49–58.

Anthes, A. R., Rosenthal, L. S. & Trout, W. J. 1971. Preliminary results from an asymmetric model for the tropical cyclone. *Monthly Weather Rev. 99*, 744–758.

Arakawa, A. 1966. Computational design for long term numerical integration of the equations of fluid motion. *Journal of Computational Physics 1*, 119–143.

Cressman, G. P. 1951. The development and motion of typhoon "Doris", 1960. *Bull. American Meteorological Society 9*, 326–333.

Grammeltvedt, A. 1969. A survey of finite-difference schemes for the primitive equations for a barotropic fluid. *Monthly Weather Rev. 97*, 384–404.

Gray, W. M. 1967. Global view of the origin of tropical disturbances and storms. *Monthly Weather Rev. 97*, 669–700.

Harlow, F. H. & Welch, J. E. 1965. Numerical calculation of time dependent viscous incompressible flow of fluid with free surface. *Phys. Fluids 8*, 2182–2185.

Hawkins, H. F. & Rubsam, D. T. 1968. Hurricane "Hilda" 1964: II. Structure and budgets of the hurricane on October, 1964. *Monthly Weather Rev. 96*, 617–636.

Hill, G. E. 1968. Grid telescoping in numerical weather prediction. *J. Applied Meteorology 1*, 29–38.

Jordan, C. L. 1958. Mean soundings for the West Indies area. *J. Meteorology 18*, 91–97.

Jordan, E. S. 1952. An observational study of the upper wind-circulation around tropical storms. *J. Meteorology 9*, 340–346.

Kuo, H. L. 1965. On formation and intensification of tropical cyclones through latent heat release by cumulus convection. *J. Atmos. Sci. 22*, 40–63.

Kurihara, Y. & Holloway, J. Jr, 1967. Numerical integration of a nine-level global primitive equations model formulated by the box method. *Monthly Weather Rev. 95*, 509–530.

Kurihara, Y. & Tuleya, R. E. 1974. Structure of a tropical cyclone developed in a three-dimensional numerical simulation model. *J. Atmos. Sci. 31*, 893–919.

Kwizak, M. & Robert, J. A. 1971. A semi-implicit scheme for grid point atmospheric models of the primitive equations. *Monthly Weather Rev. 99*, 32–36.

Lilly, D. K. 1965. On the computational stability of numerical solutions of time-dependent non-linear geophysical fluid dynamic problems. *Monthly Weather Rev. 93*, 11–26.

Madala, R. V. 1973. A three dimensional numerical model of the life cycle of a hurricane. Ph.D. dissertation, Florida State University Tallahassee. 133 pp.

Mathur, M. B. 1974. A multi-grid primitive equation model to simulate the development of an asymmetric hurricane (Isebell, 1964). *J. Atmos. Sci. 31*, 371–393.

McPherson, D. R. 1971. Note on the semi-implicit integration of a fine mesh limited-area prediction

model on an offset grid. *Monthly Weather Rev.* *99*, 242–246.
Ooyama, J. 1969. Numerical simulation of the life cycle of tropical cyclones. *J. Atmos. Sci.* *26*, 3–40.
Riehl, H. & Malkus, J. S. 1961. Some aspects of hurricane "Daisy" 1958. *Tellus 13*, 181–213.
Robert, A., Henderson, J. & Turnbull, C. 1972. An implicit time integration scheme for baroclinic models of the atmosphere. *Monthly Weather Rev.* *100*, 329–335.
Rossby, C. G. 1948. On displacement and intensity changes of atmospheric vortices. *J. Marine Research 7*, 175–187.
Rosenthal, S. L. 1964. Some attempts to simulate the development of tropical cyclones by numerical methods. *Monthly Weather Rev. 92*, 1–21.
Rosenthal, S. L. 1969. Numerical experiments with a multilevel primitive equation model designed to simulate the development of tropical cyclones, experiment 1. *National Hurricane Research Laboratory, Technical Memorandum No. 82*, p. 36.
Sundqvist, H. 1970. Numerical simulation of the development of tropical cyclones with a ten-level model. Part 1. *Tellus 22*, 359–390.
Williams, G. P. 1969. Numerical integration of the three-dimensional Navier-Stokes equations for incompressible flow. *J. Fluid Mech. 37*, 727–750.
Yamasaki, M. 1968*a*. A tropical cyclone model with parameterized vertical partition of released latent heat. *J. Meteor. Soc. Japan 46*, 202–214.
Yamasaki, M. 1968*b*. Detailed analysis of a tropical cyclone simulated with a 13-layer model. *Papers in Meteorology and Geophysics 19*, 559–585.
Yamasaki, M. 1969. Large scale disturbances in the conditionally unstable atmosphere in low latitudes. *Papers in Meteorology and Geophysics 20*, 289–336.
Yeh, T. C. 1950. The motion of tropical storms under the influence of a superimposed southerly current. *J. Meteorology 7*, 108–113.

ЧИСЛЕННОЕ МОДЕЛИРОВАНИЕ АСИММЕТРИЧНЫХ УРАГАНОВ В ПОТОКЕ С ВЕРТИКАЛЬНЫМ ПОПЕРЕЧНЫМ СДВИГОМ НА β-ПЛОСКОСТИ

Разработана трехуровенная полуявная модель для моделирования движущихся асимметричных ураганов на β-плоскости при использовании метода Куо для параметризации кучевой конвекции. В модель прямым образом включен перенос явного и скрытого тепла от океана к атмосфере. Для того чтобы предсказать движение урагана над большой областью и все же разрешить более тонкие детали вблизи его глаза, использовалась многошаговая сетка с движущейся тонкой сеткой с размером ячейки 20 *км*, окруженная двумя грубыми сетками с размерами ячеек в 60 и 180 *км*, соответственно. Сравнение результатов с вычислениями на f-плоскости показывает, что вихрь на β-плоскости усиливается с меньшей скоростью перед стадией бури, но с той же скоростью после нее. Ураган на β-плоскости был асимметричен в течение всего своего цикла жизни и эти асимметричности были похожими на те, которые наблюдаются в реальных ураганах. Вихрь движется на β-плоскости с фазовой скоростью 4,3 *км*/час для западной и 3,3 *км*/час для северной компонент. Модель интегрировалась также для двух случаев, когда начальный вихрь накладывался на основной поток, меняющийся по высоте. Результаты указывают, что сила моделируемого урагана очень резко зависит от величины сдвига скорости по вертикали для основного потока; для большого сдвига (≥ 15 *м* сек$^{-1}$/12 *км*) вихрь не был способен развиться в ураган. Вычисления показали, что взвешенная по давлению скорость основного потока между поверхностью и уровнем 12 *км* очень хорошо согласуется с величиной направляющего потока. В результате взаимодействия между циркуляций в урагане и основным потоком ураган двигался колеблющимся путем с амплитудой в 30 *км* и периодом около 20 часов.